Theory and Simulation of the Rayleigh-Taylor Instability in the Limit of Large Larmor Radius

J. D. Huba and J. G. Lyon
Geophysical and Plasma Dynamics Branch, Plasma Physics Division, Naval Research Laboratory, Washington, D.C. 20375

and

A. B. Hassam[(a)]
Science Applications International Corporation, McLean, Virginia 22102
(Received 15 June 1987)

The theory and first nonlinear simulations of the Rayleigh-Taylor instability in the limit of large ion Larmor radius are presented. It is shown that in the limit of large Larmor radius, the Rayleigh-Taylor instability evolves much faster and in a dramatically different manner than in the limit of small Larmor radius.

PACS numbers: 52.30.Gz, 47.65.+a, 52.35.Py, 52.65.+z

Interchange instabilities, such as the Rayleigh-Taylor instability, have been the subject of intense scientific interest for most of this century.[1] Generically, an interchange instability can occur when two fluids of different densities are accelerated. Although initially studied in the context of hydrodynamic theory,[2] this type of instability has also been shown to exist in magnetized plasmas.[3] Subsequently, plasma interchange modes have become an important area of research in the plasma physics community, and a considerable amount of work (theoretical, experimental, and computational) has been done over the past two decades. The bulk of the research has been motivated by the fusion research program, especially in regard to the stability of magnetically confined plasmas[4] and imploding laser target pellets.[5] However, there is also evidence that this type of instability can occur in space plasmas.[6] Thus, interchange modes are relevant to a broad spectrum of plasma regimes.

The study of the Rayleigh-Taylor instability in a magnetized plasma has largely been confined to the regime $\rho_i/L \ll 1$ and $\omega/\Omega_i \ll 1$, where ρ_i and Ω_i are the ion gyroradius and gyrofrequency, respectively, and ω and L are the frequency and length scales of interest, respectively. Standard MHD theory can be used when $k\rho_i \ll 1$ (where k is the wave number), while finite-Larmor-radius MHD theory is used when $k\rho_i \lesssim 1$.[7] (Of course, use of kinetic theory can remove all restrictions on the value of $k\rho_i$.[8,9]) However, space[10] and laboratory[11,12] experiments have observed plasma structure, apparently caused by the rapid deceleration of a plasma expanding into a strong magnetic field, in the parameter regime $\rho_i/L \gg 1$ and $\omega/\Omega_i \gg 1$ but $\rho_e/L \ll 1$ and $\omega/\Omega_e \ll 1$. Similar structure has also been observed in earlier plasma-expansion experiments[13,14] and in θ-pinch implosion experiments[15] in the regime $\rho_i/L \lesssim 1$ and $\omega/\Omega_i \lesssim 1$. The purpose of this Letter is to investigate, both analytically and computationally, the development of the Rayleigh-Taylor instability in the regime of large ion Larmor radius (i.e., $\rho_i/L \gg 1$ and $\omega/\Omega_i \gg 1$). We show that in this regime the Rayleigh-Taylor instability develops much faster and has a dramatically different nonlinear behavior than the conventional Rayleigh-Taylor instability.

A set of one-fluid, modified MHD equations has been derived which describes a plasma for arbitrary ρ_i/L or ω/Ω_i[16,17]:

$$\partial n/\partial t + \nabla \cdot n\mathbf{u} = 0, \qquad (1)$$

$$nM\, d\mathbf{u}/dt = -T\nabla n - \nabla B^2/8\pi + \mathbf{B}\cdot\nabla\mathbf{B}/4\pi + nM\mathbf{g}, \qquad (2)$$

$$\partial \mathbf{B}/\partial t = \nabla \times (\mathbf{u}\times\mathbf{B}) - (Mc/e)\nabla \times d\mathbf{u}/dt, \qquad (3)$$

where $\mathbf{u}$ is the center-of-mass velocity, n is the density, $\mathbf{B}$ is the magnetic field, M is the ion mass, and $\mathbf{g}$ is the gravitational force. (With regard to plasma-expansion experiments, we can identify the plasma acceleration with an effective gravitational acceleration, i.e., $d\mathbf{u}_0/dt = -\mathbf{g}_{\text{eff}}$.) Equations (1)–(3) are derived directly from the ion and electron Vlasov equations under the following assumptions. We assume that (1) $\rho_e/L \ll 1$ and $\omega/\Omega_e \ll 1$ (i.e., the electrons are strongly magnetized), (2) the electron and ion pressure tensors are isotropic, (3) the electron and ion fluids are isothermal with $T = T_e + T_i$, and (4) the Debye length is very small. We mention that (1)–(3) are similar to a set of one-fluid MHD equations derived by Hassam and Lee[18] in the limit $T_i = 0$.

The final term in (3) is what makes these equations different from the conventional ideal MHD equations. In this representation it is clear that ion inertia is the origin of this term and that it is potentially important when $\omega/\Omega_i \gg 1$ (or $\rho_i/L \gg 1$). We also point out that (3) can be rewritten as

$$\partial \mathbf{B}/\partial t = \nabla \times (\mathbf{u}\times\mathbf{B}) - \nabla \times (\mathbf{j}\times\mathbf{B})/ne, \qquad (4)$$

so that the new term can be identified as the Hall term.

To study the linear evolution of the Rayleigh-Taylor instability in both the small- and large-Larmor-radius limits, we consider the following slab geometry and plasma configuration. We assume $\mathbf{B}=B_0(x)\hat{\mathbf{e}}_z$, $n=n_0(x)$, and $\mathbf{g}=g\hat{\mathbf{e}}_x$. The equilibrium is given by $\partial(n_0T+B_0^2/8\pi)/\partial x=n_0Mg$. We perturb (1)-(3) about this equilibrium and assume that perturbations are proportional to $\exp[i(k_yy-\omega t)]$. We consider the "local" limit and require $k_yL_n\gg 1$, where $L_n=(\partial \ln n_0/\partial x)^{-1}$ is the scale length of the density gradient. The dispersion equation is given by[16]

$$\frac{-\omega^4}{k_y^2V_A^2}+(1+\beta)\omega^2-\left[\frac{g}{L_n}\right]\left[1-\frac{\partial \ln B_0}{\partial \ln n_0}\right]+\frac{\rho_i}{L_n}\frac{1}{k_yC_s}(\omega^2-k_y^2gL_n)\omega=0, \tag{5}$$

where $V_A=B/(4\pi nM)^{1/2}$ is the Alfvén velocity, $C_s=(2T/M)^{1/2}$ is the sound speed, $\rho_i=C_s/\Omega_i$, and $\beta=8\pi nT/B^2$.

In the limit $\rho_i/L_n\to 0$ (i.e., conventional MHD theory), we recover from (5) the magnetosonic modes $[\omega^2=k_y^2V_A^2(1+\beta)]$ and the usual Rayleigh-Taylor instability $[\omega^2=(g/L_n)(1-\partial \ln B_0/\partial \ln n_0)]$. Instability can occur when $g/L_n<0$ with the growth rate $\gamma_0=(g/L_n)^{1/2}$. However, when $\rho_i/L_n\gg 1$, a faster growing mode can occur which has a growth rate determined by $\omega^2=k_y^2gL_n$.[11,16] Again, instability can occur when $gL_n<0$ but the growth rate is $\gamma=k_y(gL_n)^{1/2}=k_yL_n\gamma_0$; the turn-on condition for this mode is $(g/L_n)(1-\partial \ln B_0/\partial \ln n_0)>\Omega_i^2/4$. Interestingly, for a magnetically confined plasma expansion in a low-β plasma, the turn-on condition is independent of the magnetic field, which is consistent with experimental observations.[12] Of further interest is the eigenmode structure. We note that when $\rho_i/L_n\gg 1$ and $\omega\sim k_yC_s$, then $\omega/\Omega_i\gg 1$ and the final term in (3) will be large unless $\hat{\mathbf{e}}_z\cdot\nabla\times\mathbf{u}\to 0$. We use this fact in the equation obtained by taking the z component of the curl of (2) to get $-i\omega(\partial n_0/\partial x)\tilde{u}_y=ik_yg\tilde{n}$. From (1) we obtain $-i\omega\tilde{n}+in_0k_y\tilde{u}_y+(\partial n_0/\partial x)\tilde{u}_x=0$. But since $\hat{\mathbf{e}}_z\cdot\nabla\times\mathbf{u}=0$ we note that $ik_y\tilde{u}_x\simeq 0$, so that $-i\omega\tilde{n}+in_0k_y\tilde{u}_y=0$. Thus, eliminating $\tilde{n}$ and $\tilde{u}_y$ from these equations we get $\omega^2=k_y^2gL_n$. The crucial point is that the fluid motion is primarily curl free and not divergence free (i.e., $\nabla\times\tilde{\mathbf{u}}=0$ and $\nabla\cdot\tilde{\mathbf{u}}=ik_y\tilde{u}_y\neq 0$). This represents a behavior quite different from the conventional MHD Rayleigh-Taylor instability which is primarily divergence free and not curl free ($\nabla\cdot\tilde{\mathbf{u}}=0$ and $\nabla\times\tilde{\mathbf{u}}\neq 0$).

This contrasting fluid behavior can also be seen by considering the following simplified ion momentum equation in the limit $T\to 0$: $nM\,d\mathbf{V}_i/dt=e(\mathbf{E}+\mathbf{V}_i\times\mathbf{B}/c)$. In the latter case, when $\omega/\Omega_i\ll 1$, the dominant perturbed ion velocity is $\tilde{\mathbf{V}}_i=-c\tilde{\mathbf{E}}\times\mathbf{B}/c$ which is divergence free. In the former case, when $\omega/\Omega_i\gg 1$, the dominant perturbed ion velocity is $\tilde{\mathbf{V}}_i=ie\tilde{\mathbf{E}}/nM\omega$ which is curl free. Thus, on the basis of this linear eigenfunction we anticipate that the nonlinear behavior of the unmagnetized and magnetized ion Rayleigh-Taylor instabilities will be quite different.

We now confirm this suspicion by presenting results of 2D numerical simulations of the Rayleigh-Taylor instability in both the limit of small Larmor radius (i.e., magnetized ions) and the limit of large Larmor radius (i.e., unmagnetized ions). We solve (1), (2), and (4) numerically on a Cartesian grid with resolution 125×100 (x,y). We consider plasma motion only in the plane transverse to the magnetic field ($\mathbf{B}=-B\hat{\mathbf{e}}_z$). Hard-wall boundary conditions were used in the x direction, while periodic boundary conditions were used in the y direction. The algorithm used solves (1), (2), and (4) in conservation form using a total variation decreasing nonlinear switch between a first-order transport scheme and an Adams-Bashforth, centered eighth-order spatial scheme.[19] The following density profile was chosen: $n_0(x)=0.55+0.45\tanh(x/L_2)$ for $x<0$, and

$$n_0(x)=[0.55+0.45\tanh(x/L_2)]\exp(-x/L_1)$$

for $x>0$, with $\mathbf{g}=-g\hat{\mathbf{e}}_x$ and $\mathbf{B}(x)$ determined from equilibrium force balance. We choose $L_1=1.0$, $L_2=0.2$, $C_s=1.0$, and $g=1.0$. The length scale is normalized to $L_1=1.0$, the velocity is normalized to $C_s=1.0$, and the time scale is normalized to $L_1/C_s=1.0$. The boundaries used in the simulations are $x=-2.5$ and 2.5, and $y=0.0$ and 4.0.

We benchmarked the code in the linear regime by initializing the grid with a single mode and calculating the eigenfunction and eigenvalue. For $\rho_i/L_2=0$ and $\lambda_x=0.8$, we calculate the linear growth rate to be $\gamma\simeq 1.70$, which agrees well with the theoretical value of $\gamma\simeq 1.81$. In the nonlinear regime it is difficult to benchmark the code with previous results because the code is compressible and we treat a diffuse density profile (as opposed to a sharp-boundary model). Nevertheless, we estimate the Froude number to be $F\simeq 0.27$ which is in reasonable agreement with experimental[20] ($F\simeq 0.2$–0.3) and numerical[21] ($F\simeq 0.23$) results. The initial conditions for the simulations discussed in the remainder of the Letter is a 1% random density fluctuation throughout the grid.

In Fig. 1 we show the density contours [Fig. 1(a)] and velocity vector field [Fig. 1(b)] for the Rayleigh-Taylor instability in the small-Larmor-radius limit (i.e., we use $\rho_i/L_2=0$) at $t=5.5$. We show these results primarily for comparison with the Rayleigh-Taylor instability in the large-Larmor-radius limit. The following points should be noted. First, the instability initially develops in the region $x<0.2$. The peak of the density at $t=0$ is at

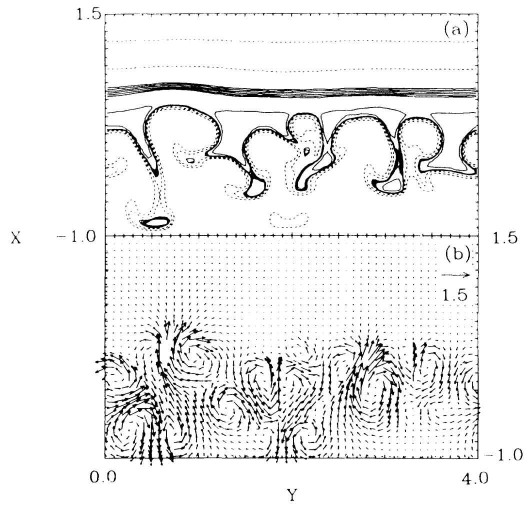

FIG. 1. Simulation results for the Rayleigh-Taylor instability in the limit of small Larmor radius ($\rho_i/L_2=0$) at time $t=5.5$. The magnetic field is in the $-z$ direction (out of the page). (a) Density contours. The contour levels are as follows: dashed lines (0.30 and 0.43), heavy solid lines (0.55), and light solid lines (0.68 and 0.80). (b) Velocity vector field. The "unit" velocity vector of 1.5 is shown for comparison.

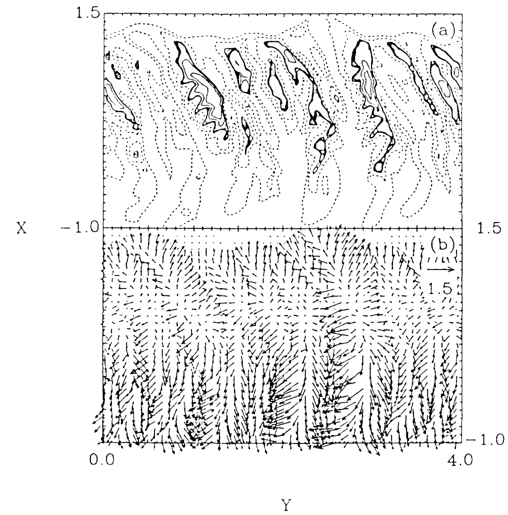

FIG. 2. Simulation results for the Rayleigh-Taylor instability in the limit of large Larmor radius ($\rho_i/L_2=5$) at time $t=1.0$. The magnetic field is in the $-z$ direction (out of the page). (a) Density contours. The contour levels are the same as in Fig. 1(a). (b) Velocity vector field. The "unit" velocity vector of 1.5 is shown for comparison.

$x=0.2$ so that the linearly unstable regime is $x<0.2$ where $g\,\partial \ln n_0/\partial x<0$. As the instability evolves nonlinearly, we find that the usual "spike" and "bubble" morphology develops [see Fig. 1(a)].[22] The "heavy" material falls (i.e., the spike) while the "light" material rises (i.e., the bubble). In each case, a mushroomlike structure develops. Second, associated with the development of the mushroomlike heads is the development of counterrotating vortices. This is evident in Fig. 1(b). The fluid motion in the spikes is such that the fluid falls downward in the center of the spikes, but at the edges is deflected horizontally, and eventually turns upwards creating a swirling pattern. The bubbles display the same behavior, but the upward-flowing fluid is eventually turned around to go downward. Thus the fluid has a significant curl as expected. And third, the bulk of the "action" takes place in the linearly unstable region (i.e., $x<0.2$). We see that disturbed fluid motion occurs between $x\simeq-1.0$ and $x\simeq0.7$ so by this time there is relatively little disruption of the "stable" side of the density profile (i.e., where $g\,\partial \ln n_0/\partial x>0$).

In Fig. 2 we show the density contours [Fig. 2(a)] and velocity vector field [Fig. 2(b)] for the Rayleigh-Taylor instability in the limit of large Larmor radius (i.e., we use $\rho_i/L_2=5.0$) at $t=1.0$. The following points should be noted. First, it is clear that the unmagnetized Rayleigh-Taylor instability develops much faster than the magnetized Rayleigh-Taylor instability, consistent with linear theory. Second, although not evident in Fig. 2, we find that during the linear evolution of the unmagnetized instability, the fastest growing modes are the shortest-wavelength modes. This is consistent with the theoretical analysis which indicated that $\gamma\propto k_y$. However, longer-wavelength structures seem to dominate as the instability progresses, i.e., those that are comparable to the initial density-gradient scale length. Third, the instability initially develops on the "unstable" side of the density profile (i.e., $g\,\partial \ln n_0/\partial x<0$), but unlike the magnetized instability, it disrupts more of the density profile [see Fig. 2(a)]. The extent of the disruption is between $x\simeq-1.1$ to $x\simeq1.6$, a significantly larger region than the previous case. It appears that narrow channels develop which allow the magnetic field to penetrate into the stable top side of the density profile. Fourth, a secondary instability appears to develop on one side of the largest density enhancements, i.e., the "fishbonelike" structure in Fig. 2(a). It is not entirely clear what causes this finer scale structure; it may be an eigenmode structure or a secondary instability. Fifth, the velocity vector field is completely different from the magnetized-ion case. The flow is clearly not divergence-free [see Fig. 2(b)] and large-scale flows seem to form fluid "sheets." The maximum velocity reached in this case is $u_m=1.9$ which is somewhat larger than the "free-fall" velocity $u=1.5$. And finally, we add that we have also performed simulations for $\rho_i/L_2\simeq1$; the linear growth rate of the instability is smaller than either of the two examples presented above, in accordance with linear theory.[16]

In conclusion, we have presented the theory and first nonlinear fluid simulations of the Rayleigh-Taylor instability in the limit of large ion Larmor radius (i.e., $\rho_i/L \gg 1$). These results are based upon a modified set of one-fluid MHD equations which is valid for arbitrary values of ρ_i/L or ω/Ω_i (but requires $\rho_e/L \ll 1$ and $\omega/\Omega_e \ll 1$). We have demonstrated that in this limit the Rayleigh-Taylor instability evolves in a dramatically different manner from the conventional, small-Larmor-radius Rayleigh-Taylor instability. Besides developing much faster, the unmagnetized instability appears to be more disruptive of an accelerating plasma density shell, and generates compressible ion flows. Moreover, although the fastest-growing modes have the shortest wavelength, longer-wavelength modes seem to dominate in the nonlinear regime. Finally, these results are consistent with the observed structuring of the Active Magnetospheric Particle Tracer Explorer (AMPTE) barium release in the magnetotail,[10] and recent laboratory observations of plasma structure.[12] In both cases, plasma shells rapidly decelerate as they expand into a strong magnetic field, develop structure on time scales much faster than the ion cyclotron period, and are dominated by structure sizes comparable to the density-gradient scale length.

We thank Dr. B. Ripin for helpful discussions regarding the Naval Research Laboratory laser experiment and for pointing out the experimental observation that the onset of instability is independent of magnetic field strength above a critical value. We also thank Dr. P. Bernhardt for discussions regarding the Active Magnetospheric Particle Tracer Explorer data and Dr. H. Rowland for assistance in benchmarking the code. This research has been supported by the Defense Nuclear Agency.

[a]Permanent address: University of Maryland, College Park, MD 20742.

[1]S. Chandrasekhar, *Hydrodynamic and Hydromagnetic Stability* (Dover, New York, 1961), p. 428.

[2]Lord Rayleigh, *Scientific Papers* (Cambridge Univ. Press, London, 1900), Vol. ii, p. 200.

[3]M. Kruskal and M. Schwarzchild, Proc. Roy. Soc. London A **223**, 348 (1954).

[4]C. L. Longmire and M. N. Rosenbluth, Ann. Phys. (N.Y.) **1**, 120 (1957).

[5]S. E. Bodner, Phys. Rev. Lett. **33**, 761 (1974).

[6]G. L. Siscoe, in *Solar-Terrestrial Physics,* edited by R. L. Carovillano and J. M. Forbes (Reidel, Boston, 1983), p. 11.

[7]K. V. Roberts and J. B. Taylor, Phys. Rev. Lett. **8**, 197 (1962).

[8]M. N. Rosenbluth, N. A. Krall, and N. Rostoker, Nucl. Fusion, Suppl. **1**, 143 (1962).

[9]S. P. Gary and M. F. Thomsen, J. Plasma Phys. **28**, 551 (1982).

[10]P. A. Bernhardt, R. Roussel-Dupré, M. B. Pongratz, G. Haerendel, A. Valenzuela, D. A. Gurnett, and R. R. Anderson, to be published.

[11]S. Okada, K. Sato, and T. Sekiguchi, Jpn. J. Appl. Phys. **20**, 157 (1981).

[12]B. H. Ripin, E. A. McLean, C. K. Manka, C. Pawley, J. A. Stamper, T. A. Peyser, A. N. Mostovych, J. Grun, A. B. Hassam, and J. D. Huba, Phys. Rev. Lett. **59**, 2299 (1987).

[13]H. Dickinson, W. H. Bostick, J. N. DiMarco, and S. Koslov, Phys. Fluids **5**, 1048 (1962).

[14]G. Jellison and C. Parsons, Phys. Fluids **24**, 1787 (1981).

[15]M. Keilhacker, M. Kornherr, H. Niedemeyer, F. Soldner, and K.-H. Stever, Phys. Rev. Lett. **32**, 1044 (1974); K. F. McKenna, R. Kristal, and E. L. Zimmerman, Phys. Fluids **18**, 1371 (1975).

[16]A. B. Hassam and J. D. Huba, Geophys. Res. Lett. **14**, 60 (1987).

[17]A. B. Hassam and J. D. Huba, to be published.

[18]A. B. Hassam and Y. C. Lee, Phys. Fluids **27**, 438 (1984).

[19]A. Harten, J. Comput. Phys. **49**, 357 (1983).

[20]H. W. Emmons, C. T. Chang, and B. C. Watson, J. Fluid Mech. **7**, 177 (1959).

[21]G. R. Baker, D. I. Meiron, and S. A. Orszag, Phys. Fluids **23**, 1485 (1980).

[22]M. H. Emery, J. H. Gardner, and J. P. Boris, Phys. Rev. Lett. **48**, 677 (1982).